

Calcite polymorphs in historic plasters of India's arid region – execution technique, composition and characterization

Shikha Bansal¹ and Manjinder Singh^{2,*}

¹National Museum Institute, Department of Conservation, Janpath, New Delhi 110 011, India

²National Research Laboratory for Conservation of Cultural Property, Sector-E/3, Aliganj, Lucknow 226 024, India

In this work, the microscopic observation of thin section was utilized to analyse the geological and fine morphological features of the 16th century Amber fort lime plaster – a World Heritage site. FTIR, XRD and SEM photomicrographs showed the stabilization of different crystalline phases of calcite polymorphs. Chemical analysis and SEM-EDX data revealed dolomitic limestone was probably sourced for plaster works. The high magnesium present in the raw material, the environmental conditions during the application, pH, etc. have stabilized calcite polymorphs in the plaster. The calcite meta-stable phases have undergone dissolution with time making the plaster weak. This has increased porosity, permeability, and resultant lowering of plaster's mechanical strength. Thermal analysis and cementation index revealed use of non-hydraulic, binder-rich, air-lime for plaster works. The granulometric study showed the mixing of reddish-brown sand-size grains, and the aggregates were probably sourced from the same location for major construction activity. The low proportion of aggregates led to reduced mechanical strength, and the plaster is vulnerable to damage.

Keywords: Arid regions, calcite polymorphs, decorative works, heritage structures.

SIGNIFICANT variations in the composition and strength of ancient plasters and mortars are observed in different geographical locations and periods of historical construction in India^{1,2}. The preparation as well as execution techniques of lime mortar also differed in different parts of the country^{3,4}. To execute restoration work, the plasters/mortars must be extensively studied to prepare compatible and matching repair mix. Moreover, no recorded work highlights the analysis and characterization of materials used in lime works of the western Indian desert region of Rajasthan. This region was the home of great rulers, rich in monuments and havelis with beautiful lime works and decorative surfaces. Rajasthan is associated with legends of romance and bravery as well as paintings, history and architecture that go back several centuries. The decorative art on lime plaster in this region started developing in the 14th century and

was at its peak in the 16th century. The Persian colonial art also flourished in this part and the colour palette of paintings suddenly changed from vibrant red to more bright colours⁵.

The Rajasthan decorative arts stretched on shiny white plaster and the technique is known as fresco buno⁶. The plaster technique is considered similar to the true fresco of Italy. Rajasthan is also the lime capital of India and compact limestone, granular limestone, magnesia limestone, and kankar limestone are abundantly available in the state. An earlier study reported the burning of kankar limestone in a limekiln for plaster works inside the Taj Mahal in Agra⁷.

The region is mostly arid and includes rocky terrain, rolling dunes, plateaus, tracts of land filled with thorny shrubs, wetlands, river-drained plains, ravines and wooded areas. It experiences severe heat. The high evaporation rate of water due to heat and less rainfall has made the groundwater saline. Due to local climatic conditions, the technique of lime plastering practised in this region is differs from those in other parts of India. The lime works in India's desert region were executed by a unique technique locally named ala-gila⁵.

Ala-gila plastering technique

In this technique, the wall is firstly chiselled to make it uneven and rough, brushed and washed many times with water. The temperature in Rajasthan is very high; therefore, the wall is drenched with water to reduce the reaction rate of calcium hydroxide⁸. During plastering, the wall is kept semi-wet for the application of each layer of plaster. Water reduces the reaction rate of carbon dioxide with lime and increases workability.

For all plaster works, lime slaked for at least six months was used. If the lime is not well slaked and/or properly filtered, it may develop swelling or bubbles during application. The slaked lime is properly mixed with aggregates like sand, granules, brick dust and some organic binders. This mixture is stirred well to improve the cementing property, followed by adding curd and jaggery.

The first layer of the plaster is applied to the bare wet wall of stone or brick. These layers are coarser and always have large-sized aggregates. The plaster is evenly spread

*For correspondence. (e-mail: m_singh_asi@yahoo.com)

by wooden trowels, ensuring that the layer is free from pits or pores. Sometimes paddy husk or animal hairs are added to strengthen the plaster. The plaster is beaten gently with wooden trowels to make it smooth and water is sprinkled to make the surface damp. The second layer of the plaster mixed with small-sized aggregates is subsequently applied. A layer of *kara*, a mixture of pure lime and marble dust, jaggery and fenugreek seeds is applied during plaster setting. The second layer is thinner than the first layer and forms the base layer for paintings. The wet plaster is beaten regularly using wooden trowels and a churn made of lime and aggregates is applied to increase fluidity and workability. The final layer is bright, white, smooth, filtered lime paste mixed with curd and sugar in the ratio 1 : 3 for a soft and glittering finish. The final plaster is strained and filtered 3–4 times before application. The plaster is applied in several coats to give an even finish to the surface. After every wash, the surface is burnished with an agate stone for a lustrous finish. The water eventually evaporates, and on reacting with carbon dioxide, calcium hydroxide is converted into calcium carbonate. The detailed decorative figures are outlined on the top layer to be filled with colours.

Lime, a major binder, has been extensively used in ancient Indian constructions. The identified polymorphs of lime are calcite, aragonite and vaterite. The thermodynamically most stable polymorph of lime is calcite and the least stable is vaterite^{9,10}. Aragonite with its needle-like crystals and vaterite with polycrystalline spherulite structures are metastable phases of calcite. In contact with rainwater, the polymorphs of calcite start decaying till it reaches equilibrium. Any dissolved CO₂ in the rainwater will promote the dissolution of calcium polymorphs. The dissolution of metastable phases will result in increased porosity and permeability lowering the mechanical strength of ancient plaster works. The process also changes the aesthetic appearance of the outer plaster layer.

The most stable polymorph, calcite, is formed from the metastable phase of vaterite. The thermodynamically more stable calcite is preferentially formed. However, previous studies reveal that the presence of inhibitors and other ions may preserve the thermodynamically less stable aragonite and/or vaterite^{11,12}. Magnesium, either from dolomitic lime or as an impurity in lime works, will support the stabilization of aragonite¹³. The ancient plaster with needle-shaped aragonite crystals needs special protection as aragonite is more vulnerable to leaching than calcite¹⁴. Moreover, calcium carbonate and its polymorphs are not neutral and give an average pH of around 9.9.

Therefore, the lime plaster restoration of ancient heritage structures demands advanced material analysis for a better understanding. Only the instrumental analysis of historic lime may better indicate the plaster composition to plan future conservation and restoration efforts. The lime plaster samples from Amber Fort in Jaipur, Rajasthan have been studied for the chemical and mineralogical composition to

prepare a compatible plaster. The geological and micro-morphological features of the lime plaster were studied using petrological and mineralogical analysis. The instrumental techniques of X-ray fluorescence spectroscopy (XRF), X-ray diffraction (XRD), thin section, SEM (scanning electron microscope)-energy dispersive X-ray analysis were used to study the plaster composition. The purity and hydraulicity of the plaster were determined through thermal analysis. The lime plaster of the Amber Fort has been significantly damaged. This study may help prepare a compatible plaster for the planned conservation of this monument.

The Amber Fort

The Amber Fort, a 16th century world heritage monument in Rajasthan, was constructed in the reign of Raja Man Singh. Situated at the foothill entrance of the state capital Jaipur, the Fort is surrounded by many water bodies and attracts a large number of visitors every year. Figure 1 shows a general view of the Amber Fort. Jaipur city experiences hot summers with an average temperature of around 45°C in June and cold winters in January (10°–12°C) with daily sunshine. The wettest month is August, with an average rainfall of 227 mm. The Fort with architectural embellishments has decorative arts on lime plaster. The lime plaster is primarily seen in the walls and ceiling. The main building material is local sandstone blocks and fired bricks cemented with lime mortar. The lime plaster samples were collected from the exterior walls of Man Singh Mahal which have been extensively damaged. Plaster samples were also collected from a room still untouched and badly damaged due to vandalism.

Materials and methods

All the samples were collected from various points of the monuments showing damaged lime plaster. Sampling was done with the help of a small chisel and any contamination was rejected. A total of five samples were extracted from various points of the monuments for analytical examination.

As samples of lime plaster are heterogeneous, a thin section was prepared to examine mineralogical composition. For this, samples 1 and 2 were dried at 80°C for 8 h. It ensured the complete removal of inner moisture that also helped prepare crack-free thin sections. The sample was initially impregnated in low viscous resin under vacuum and subsequently, a thin section of 30 µm was prepared by grinding and polishing with zero-grade emery paper. The petrological microscope (Carl Zeiss JENAPOL) at 10× magnification was used for the optical examination of the samples. The analysis was performed at the Geo-archaeological Laboratory of Atomic Mineral Directorate, Department of Atomic Energy, New Delhi. The mineralogical

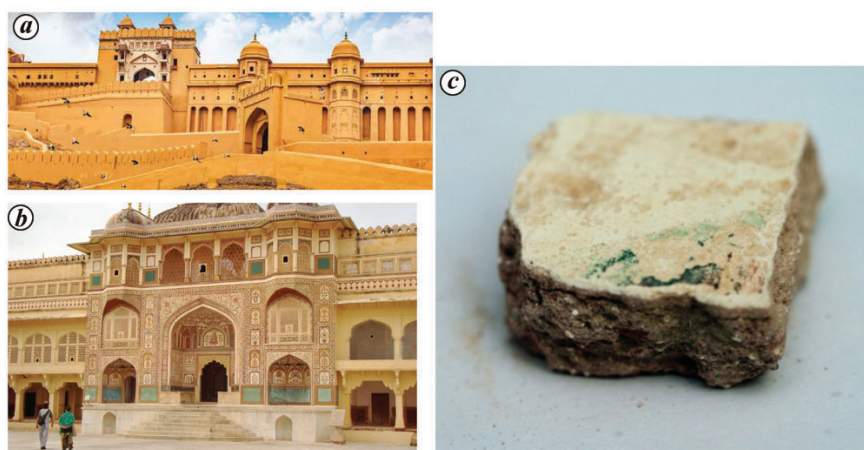


Figure 1. *a, b*, General view of Amber Fort, Jaipur. *c*, Stereo microscopic image of lime plaster showing stratigraphy of layers.

composition was studied to identify the aggregate grains and minerals present in the plaster¹⁵. The plaster samples were also examined using an electronic particle size analyser for the content of clay, silt and sand-sized particles.

To understand the stratigraphy of the layers, the samples were cut and impregnated in low viscous resin for 12 h. The embedded samples were ground and polished to achieve the required smoothness. The cross-section was studied under a stereo microscope (SM 2800 N) in the magnification range 50×–100× at Stitching Restauratie Atdier Limburg, The Conservation Institute, The Netherlands.

For the particle size analysis, the plaster samples were digested in a 25% HCl solution for 30 min, followed by mechanical stirring for 5 min.

Chemical composition analysis is an essential factor for the characterization of historic plasters^{15,16}. The chemical composition of the plasters was determined at the Advance Instrumentation Research Facilities (AIRF), Jawaharlal Nehru University, New Delhi using an XRF instrument (PAN analytical Epsilon 5). The samples were ground to a fine powder and pressed in a small crucible before placing them in XRF. Three measurements for XRF analysis were done and the data were averaged.

For loss of ignition (LOI), the samples were heated at 900°C using a muffle furnace. The parameters like hydraulicity index (HI) and cementation index (CI) of the plaster were estimated according to the equations of Jan Elsen *et al.*¹⁷ and Boynton¹³ respectively.

The minerals present in the binder and filler in the plaster were studied using XRD (PAN Analytical Xpert PRO single-crystal XRD). The instrument operating parameters were 40 keV, 40 mA current using Ni filter at room temperature with an optimized diffraction angle range of 5°–90° (2 θ).

For the microstructure, texture and composition of the plaster samples, a field-emission scanning electron microscope (MIRA3 TSCAN) equipped with a high brightness Schottky emitter for better resolution and low noise was

used. The plaster samples were mixed on aluminium stubs with the help of a carbon tape and the surface was gold-coated. SEM images were captured at various magnifications, and SEM in combination with EDS identified the elemental composition of the plaster. The Central Building Research Institute (CBRI), Roorkee facilities were used for SEM-EDX analysis of the plaster.

FTIR spectra of the plaster samples were recorded using a spectrometer (Nicolet IS50) equipped with a nitrogen-cooled MCT detector. KBr pellet technique was used for FTIR spectroscopy. FTIR analysis was carried out at the Indian Institute of Technology, Delhi in the spectral range of 400–4000 cm⁻¹.

The thermal analyser (Perkin Elmer Diamond Model) at CBRI was used for differential thermal analysis (DTA)/thermo gravimetry analysis (TGA) of plaster samples. These analyses were done by heating the test and inert reference samples under identical conditions and recording the temperature difference between them. This temperature difference was plotted against temperature, and exothermic or endothermic changes were recorded relative to an inert reference.

Results and discussion

Plastering technique

As shown in Figure 1 *c*, the plasters have been applied in three layers. The innermost plaster layer is mostly coarse, grey, with a thickness related to the topography of the stone/brick wall. The middle plaster layer is a mixture of fine and coarse aggregates in a lime binder and organic additives in the form of husk. The topmost layer, a pure lime with organic adhesives is bright and shining with or without polychromy. The cross-sectional image of the plaster under a stereomicroscope at 50× magnification depicts the three layers of the plaster. The aggregates embedded in the lime matrix are seen in the cross-section image. The heterogeneous

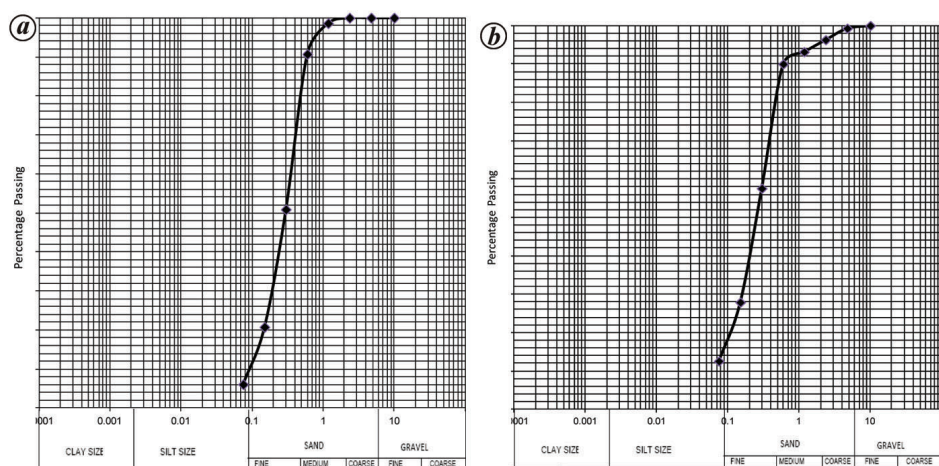


Figure 2 a, b. Grain size distribution curves of aggregates in the lime plaster samples 1 and 2.

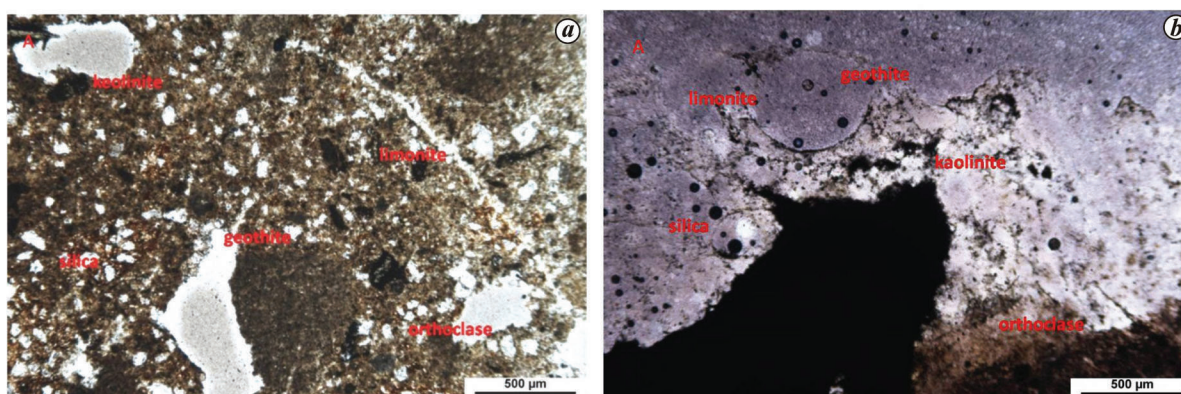


Figure 3 a, b. Thin-section image of plaster samples 1 and 2.

distribution of marble grains in the plaster is also seen. Mixing marble dust of varied grain sizes is a common technique for preparing lime plasters in western Rajasthan. The inner plaster layer has suffered the most damage due to ageing and deterioration. This layer has detached from the original wall in many places and found deteriorated. The aggregates present are usually of different sizes and shapes, consisting of local sand or rock fragments added for strength and stability of the plasterworks.

Grain size analysis of the plaster

Figure 2 a and b shows the grain size distribution curves of aggregates in the lime plaster sample. The electronic particle size analyser detects the proportion of sand, silt and clay-sized particles mixed as aggregates in the plaster. The distribution of particle size indicates that the plaster mainly consists of sand-sized particles as fine, medium and coarse grains. Since the plaster has mainly sand-sized particles, the aggregates are not well graded. A well-graded aggregate may combine two or more uniformly graded fra-

ctions. The unsorted aggregate grains are polygonal, angular to sub-angular in shape mixed during lime preparation. Most of the aggregates are greyish-brown to reddish-brown in colour. Aggregates are mostly fine-to-coarse-grained particle of diameter up to 1.18 mm in some samples. Few aggregates show porous nature, which is responsible for the reduced strength of the plaster. Moreover, the large-sized aggregate grains help better carbonate lime due to access to atmospheric carbon dioxide during carbonation. The sandy, alkaline and calcareous soils are found in this area, and aggregates are mostly derived from the local geographical region.

Petrological analysis of thin section

Figure 3 a and b shows thin-section images of the plaster samples 1 and 2. The plaster is a mixture of clay mainly from kaolinite, calcite and ferruginous cement, i.e. goethite and limonite. Silica in the form of a chart is observed in patches. The samples show reddish-brown colour due to the presence of goethite which also acts as binding material.

Table 1. Chemical composition (wt%) of plaster samples 1–5, Amber Fort, Jaipur

Sample no.	SiO ₂	Al ₂ O ₃	Fe ₂ O ₃	CaO	MgO	Na ₂ O	K ₂ O	P ₂ O ₅	TiO ₂	MnO	Loss of ignition
1	10.73	2.39	2.41	36.24	6.4	0.31	1.40	0.18	0.25	0.2	38.54
2	9.24	2.9	3.18	36.8	10.4	0.14	0.8	0.35	0.32	0.03	35.7
3	10.4	3.2	2.49	36.2	11.78	0.27	0.9	0.14	0.28	0.08	34.05
4	10.16	2.16	2.38	37.8	10.66	0.15	1.14	0.48	0.48	0.07	34.03
5	9.15	3.18	2.74	36.9	15.12	0.81	0.80	0.81	0.7	0.4	29.09

Table 2. Various components of the plasters

Sample no.	CaO + MgO	R ₂ O ₃	MgO/CaO	Hydraulicity index	Cementation index	CaO/SiO ₂
1	42.64	15.53	0.18	0.36	0.80	3.37
2	47.20	15.32	0.28	0.32	0.66	3.98
3	48.08	16.09	0.32	0.33	0.71	3.48
4	48.46	14.70	0.28	0.30	0.67	3.72
5	52.02	15.07	0.41	0.29	0.59	4.02

The coarse-grained marble-stone lining is more prominent than the orthoclase feldspar. The orthoclase particles have a relatively medium texture and are somewhat weathered. The yellow-coloured quartz grains are relatively medium in texture and slightly to moderately weathered. The oolitic orthoclase feldspar is partly surrounded by a thin coat of finely textured iron oxide.

Quartzites mostly occur in the north and east of Jaipur town. These quartzites are sedimentary and exclusively composed of medium- to fine-grained clastic quartz with minor feldspar and muscovite. The colour is white to light pink with reddish to dark brown stains of iron oxide. The cementing material is secondary silica. Examination under a microscope reveals that the quartzites are not equigranular, medium-grained rocks made up of poorly sorted subhedral to anhedral quartz. Quartz grains show deformational features such as serrated grain boundary and undulate extension. Binding calcite and aragonite are also seen in the thin section.

Composition of the plaster

Table 1 shows the chemical composition of plasters in the form of principal oxides. Calcite forms a significant component of the plaster, and CaO content varies between 36.20 and 37.80 wt%, while silicon dioxide forms around 9.15–10.73 wt% of the plaster. Another major component is magnesium oxide, whose concentration varies between 6.45 wt% and 15.20 wt% in the plaster, attributing to the exploitation of dolomitic limestone as raw material for the preparation of lime. The northwestern part of Rajasthan is the lime capital of India. According to a report published by the Indian Bureau of Mines¹⁸, the lime produced in Rajasthan is dolomitic. The CaO + MgO composition of the studied plaster varied between 42.64 wt% and 52.02 wt%, which is close to 50% of the binder (Table 2). Al₂O₃ was

always low (2.16–3.18 wt%) and total R₂O₃ varied between 14.70 and 16.09 wt% (Table 2). The data indicate that the aggregate for the Amber Fort plaster was mostly sourced from the same location, and less addition of aggregates into the plaster reduced the mechanical strength and made the plaster vulnerable to damage. Extensive damage observed at various locations of the monument is probably due to inherent problems in plaster preparation.

For the role of magnesium compound in the Amber Fort plaster, data are presented as MgO/CaO ratio, with the values varying between 0.18 and 0.41 (Table 2). The dolomitic limestone with 15% magnesium was sourced for the plaster. Magnesium oxide in considerable amounts has stabilized aragonite during the carbonation reaction of the plaster¹⁹. It has been observed that dolomitic plaster or the plaster having high magnesium content is at damage if it gets wet. The seasonal rainfall and low strength of the plaster have caused considerable damage to ancient lime works and need urgent restoration. Table 2 also lists the CI values determined using the equation of Boynton¹³. As the CI values are in the range 0.59–0.80, the Amber Fort plasters are non-hydraulic aerial lime binders. The HI values lie between 0.29 and 0.36, revealing the non-hydraulic nature of the plaster. The CaO/SiO₂ ratio lies between 3.37 and 4.02 (Table 2). For most samples, this ratio is very high compared to the desired value of 0.33 for moderate strength plaster^{20,21}. The lime/silica ratio of the studied plaster points to its compositional uniformity and low mechanical strength, making it vulnerable to damage due to physical factors. Further, the chemical composition of the plaster also indicates obtaining raw materials from the same sources during plaster preparation.

An earlier study has shown that all magnesia must be hydrated fully, as any unhydrated component may form a weak plaster that can be easily damaged²². The presence of magnesia in hydrated lime also imparts some degree of plasticity to the plasterworks.

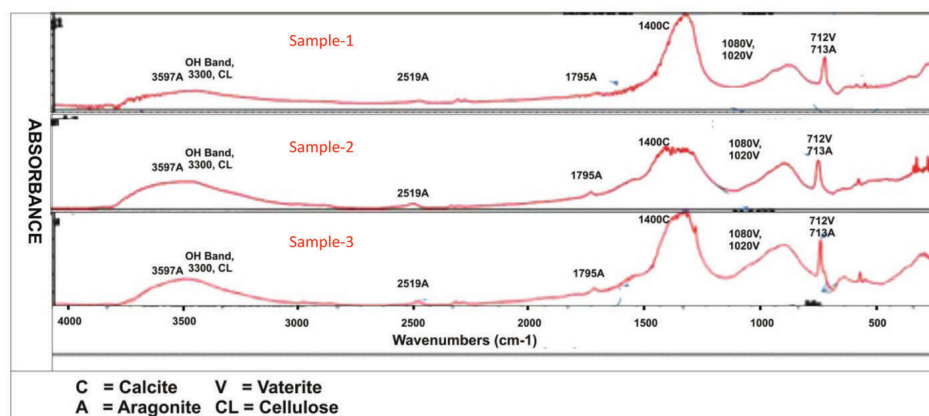


Figure 4. FTIR spectra of lime plaster samples 1–3.

FTIR analysis

Figure 4 shows the FTIR spectra of the Amber Fort plaster. A strong band centred around 3300 cm^{-1} is due to the OH group stretching. A peak around 1080 cm^{-1} in the spectra is due to plagioclase feldspar in the plaster. The characteristic FTIR peaks of lime are seen at 1400 and 712 cm^{-1} . The peak for calcite at 712 cm^{-1} has merged with the characteristic peak of aragonite at 713 cm^{-1} in the spectra. The other peaks of aragonite at 1795 , 2519 and 3597 cm^{-1} are visible in the spectra, indicating its presence in the plaster. The peaks centred around 1020 and 1084 cm^{-1} denote the presence of vaterite in the plaster^{23,24}.

XRD analysis

Figure 5 shows the X-ray diffractograms of plaster samples 1–5. Petrological analysis reveals the inclusion of marble powder as aggregate during application of the plaster. However, XRD cannot distinguish carbonates from the aggregates and lime binder. Also, it cannot detect the amorphous phase like calcium silicate hydrate in the plaster. The only detection allowed through XRD is the crystalline phase resulting from carbonation and hardening²⁵. However, XRD is a more accurate technique for identifying calcite polymorphs (calcite, aragonite and vaterite) as well as carbonation of lime^{26,27}. Figure 5 reveals that the plaster contains polymorphs of CaCO_3 (calcite, aragonite and vaterite) as binding materials. These calcite polymorphs have stabilized themselves in the plaster during carbonation on account of suitable conditions for its stabilization. Magnesium carbonate in the plaster has stabilized aragonite in the lime matrix. However, owing to its poor crystallinity, dolomite could not be recognized by XRD²⁸. Besides quartz and calcite, XRD also detected anorthite and illite in the plaster. Traces of calcium silicate hydrate and calcium aluminate hydrate were not identified through XRD in the plaster owing to their amorphous state^{28,29}. It has been reported that illite

occurs as an altered product of muscovite and feldspar in a hydrothermal environment³⁰ and with increasing temperature, illite transforms into clay³¹.

The phase transition of CaCO_3 is mostly favoured by pH of the lime mix, temperature of the mixture, degree of supersaturation and ion concentration of the mix, pressure and amount of additives, etc. used in the lime mix^{12,32}. Previous studies have shown the transformation of vaterite into stable calcite under high CO_2 pressure and alkaline pH (8.5–10.5) (refs 33–35). The prolonged moist condition and subsequent drying period help the transformation of calcium. A literature survey revealed that aragonite primarily precipitates at high temperatures, $\text{pH} < 10$ and with the occurrence of magnesium and manganese ions in the mix³³. The presence of impurities may either inhibit or enhance the precipitation/dissolution process that may also favour the crystallization of specific polymorphs of calcium carbonate^{13,36}. Aragonite polymorphs dissolve easily compared to stable calcite³⁶.

SEM-EDX analysis of the plaster

FESEM was used to observe plaster samples 1–4 to understand the binder, aggregate and reaction compounds and their forms, size, texture and distribution in the plaster. Figure 6 *a–d* shows SEM photomicrographs taken at various magnifications. The enlarged area reveals very fine capillary canals between quartz grains, probably to transport pre-solved silica to adjacent pores from the contact area³⁷ (Figure 6 *d*). The most salient feature observed in the samples is the three polymorphs of calcium carbonate with different crystal structures^{23,38}. Figure 6 *a–c* shows patches of rhombohedral cleavage crystalline calcite structure. It also shows orthorhombic cleavage aragonite and hexagonal vaterite cleavage³⁹. Plagioclase feldspar is observed as a constituent of the plaster. In the SEM images, the dark green pore-fills represent biotite separating detrital grains. The presence of plagioclase and feldspar in the

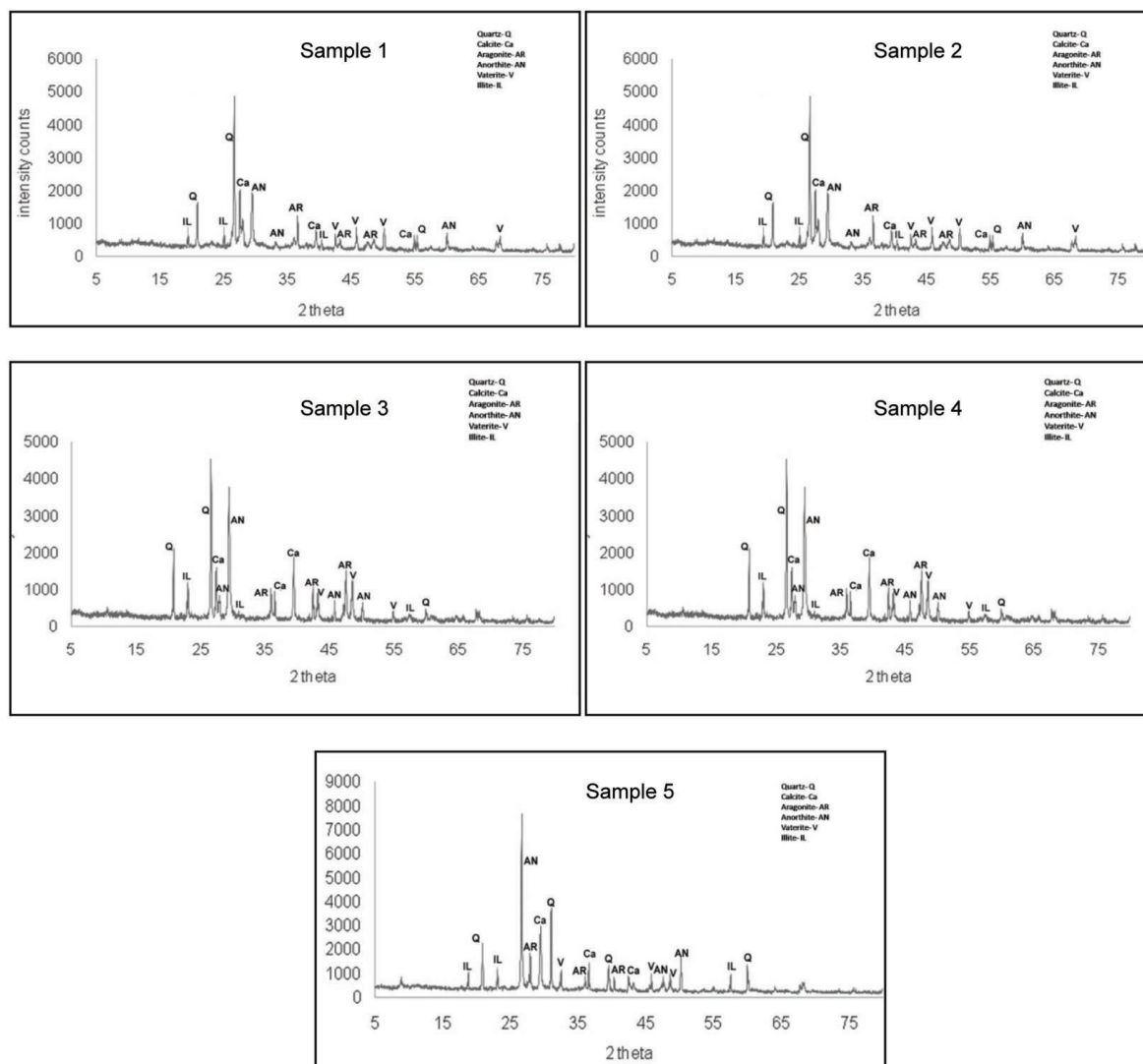


Figure 5. X-ray diffractograms of plaster samples 1–5.

Table 3. EDX data (wt%) of lime plaster samples 1–5

Sample no.	O	Si	Ca	Mg	Fe	Al	Na	Cl
1	54.14	0.73	37.84	3.96	0.99	0.30	0.85	1.20
2	52.16	23.30	7.75	8.5	–	3.85	4.47	–
3	60.57	0.16	30.38	8.49	0.14	–	0.28	–
4	59.46	0.03	32.03	8.07	0.35	–	0.06	–
5	56.30	12.10	16.60	6.60	4.10	3.10	0.73	0.10

plaster also correlates with the petrological analysis. Dolomite having poor crystallinity could not be identified under SEM and through XRD analysis of the plaster.

Table 3 shows EDX data of plaster samples 1–5. The major elements identified are Ca, Si, Al, Mg and Fe. Mg is present in the concentration range 4.76–8.75%, though magnesium carbonate was not detected in the SEM images of the plaster. Silica is low in quantity in most samples, and the studied plaster is binder-rich.

Thermal analysis of the plaster

For better characterization of the Amber Fort plaster, differential thermal analysis (DTA)-thermo gravimetry analysis (TGA) in combination with SEM and XRD was used to document the degree of hydration and carbonation of the plaster. It has been a practice to deliberately mix an extract of plant adhesives in Indian historic plaster works for strength, durability and waterproof properties⁴⁰. The organic

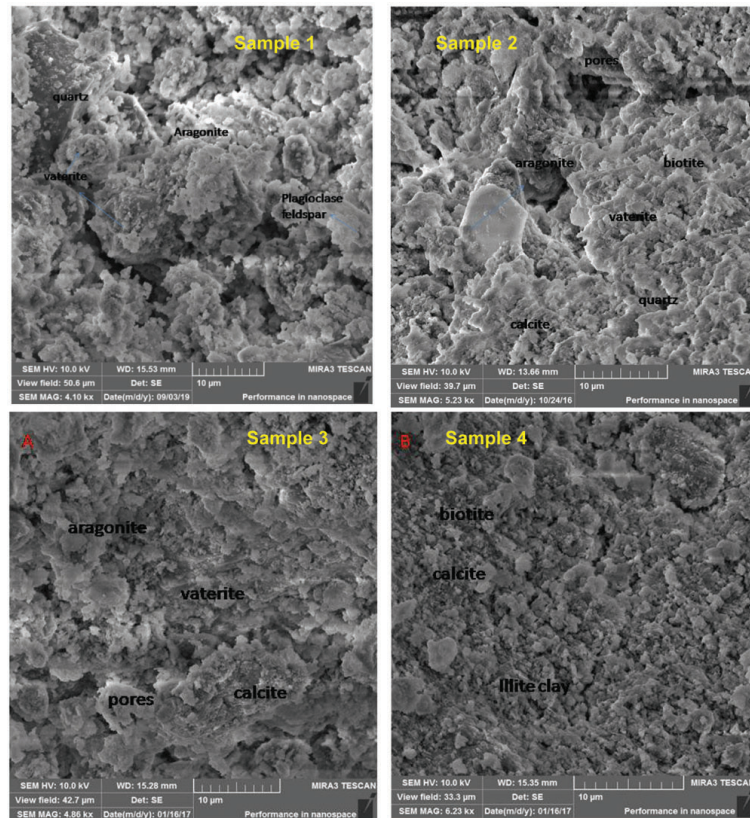


Figure 6. SEM photomicrographs of plaster samples 1–4 at different magnifications.

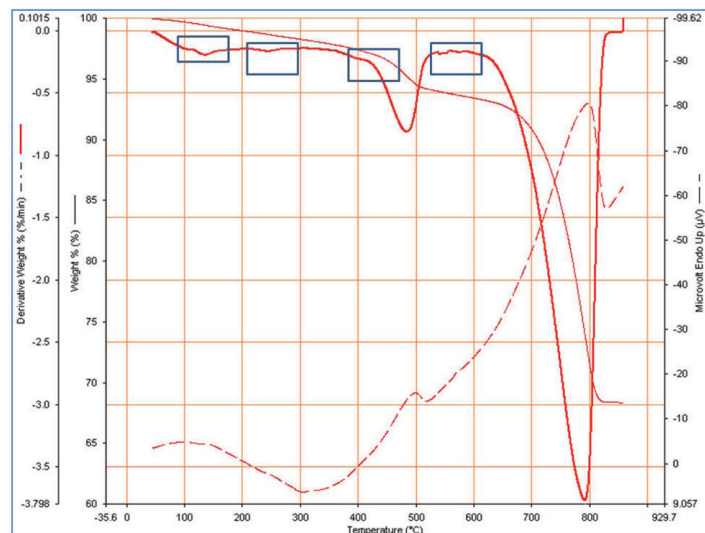


Figure 7. DTA/TGA analysis of lime plaster sample 1.

adhesive binders have changed much during the course of time, and their extraction and identification are somewhat tricky. Thermal analysis is, therefore, primarily used to gain information about plant additives, degree of hardness, carbonation reaction and lime purity.

From TGA analysis, a small weight loss of about 1.5–2% was observed at around 100°–120°C (Figure 7). This

endothermic peak represents hygroscopic water (physically absorbed water). A small endothermic peak at around 250°C is mainly attributed to chemically bound water. Another small endothermic peak around 550°–580°C is assigned to water bound to aluminosilicates. The α - to β -phase transition of quartz is also detected at around 580°C. The most important goal of thermal analysis is to distinguish between

the various polymorphs of calcite. Calcite and aragonite have been discriminated based on non-reversible phase change occurring around 470°C for aragonite⁴¹. The decomposition temperature of magnesium carbonate is in the range 450°–520°C and any calcium carbonate associated with magnesium carbonate decomposes in the range 700°–900°C (ref. 42). The weight loss of about 7% observed at around 470°–500°C is assigned to the decomposition of magnesium carbonate and aragonite. XRD and chemical analysis of the plaster, reveal the presence of aragonite and magnesium carbonate respectively. The distinctive endothermic peak of pure calcium carbonate is at around 840°C and this position changes slightly depending on the grain size, crystallinity and environmental conditions during the setting process. The weight loss of about 38% observed in the temperature range 700°–800°C indicates the loss of CO₂ from pure CaCO₃ due to some cementation material in the plaster. The presence of clay impurities in the original limestone contributes to the formation of the calcium aluminate hydrate or calcium silicate hydrate phase, which may slightly alter the decomposition temperature of CaCO₃. DTA shows exothermic peaks around 500°C and 800°C, mainly related to the dissociation of carbonates of magnesium and calcium respectively. The plaster does not present hygroscopic behaviour since absorbed water is less than 2% on heating at 120°C.

Conclusion

The main scope of this work was to analyse the components of the lime plaster used in the 16th-century Amber Fort in Rajasthan. The chemical and SEM-EDX analyses denote the sourcing of dolomitic limestone as raw material for the plaster. The environmental conditions at the time of plaster application, high magnesium content, pH, etc. have preserved the polymorphs of CaCO₃ in the plaster. The metastable polymorph phases have decayed and weakened the plaster. The aggregates are mostly sand-sized grains and their low proportions have resulted in a weak plaster vulnerable to damage. The thermal, thin-section and SEM analyses showed altered feldspar and illite clay in the plaster. A non-hydraulic air lime was used for the plaster works and the source of aggregates remained the same. The main damage-causing factors for plaster are salty water and large temperature variation. To the best of our knowledge, there are no previous reports on the composition and characterization of lime plaster from the desert region of Rajasthan that may help in restoration work.

1. Singh, M., Vinodh Kumar, S. and Waghmare, S. A., Characterization of 6–11th century AD decorative lime plasters of rock cut caves of Ellora. *Constr. Build. Mater.*, 2015, **98**; doi: 10.1016/j.conbuildmat.2015.08.039.
2. Singh, S. K., Dighe, B. and Singh, M. R., Characterization of 12th-century brick-lime stepwell plasters from New Delhi, India. *J. Archaeol. Sci. Rep.*, 2020, **29**, 102063.

3. Singh, M. R. and Kumar, S. V., Architectural features and characterization of 16th century Indian Monument Farah Bagh, Ahmed Nagar, India. *Int. J. Archit. Herit.*, 2019, **26**(2), 184–200.
4. Singh, S. K. and Singh, M., The mineralogical and physical behavior of brick aggregates in twelfth century brick-lime stepwell plasters of Gandhak-ki-baoli, New Delhi. *J. Archit. Conserv.*, 2020, 1–17.
5. Chaitanya, K., *History of Indian Painting: Rajasthani Traditions*, Abhinav Publications, 1992, pp. 50–55.
6. Pratap, R., *The Panorama of Jaipur Paintings*, DK Printworld, 1996; ISBN 10:8124600686/ISBN 13:9788124600689.
7. Aslam, M., Studies on Taj Mahal plasters. *Stud. Conserv.*, 1990, **35**(2), 102–106.
8. Mora, P., Mora, L. and Philippot, P., *The Conservation of Wall Paintings*, 1984.
9. Xyla, A. G., Mikroyannidis, J. and Koutsoukos, P. G., The inhibition of calcium carbonate precipitation in aqueous media by organophosphorus compounds. *J. Colloid Interface Sci.*, 1992, **153**(2), 537–551.
10. Tzotzi, C., Pahiadaki, T., Yiantsios, S. G., Karabelas, A. J. and Andritsos, N., A study of CaCO₃ scale formation and inhibition in RO and NF membrane processes. *J. Membr. Sci.*, 2007, **296**(1–2), 171–184.
11. Antony, A., Low, J. H., Gray, S., Childress, A. E., Le-Clech, P. and Leslie, G., Scale formation and control in high pressure membrane water treatment systems: a review. *J. Membr. Sci.*, 2011, **383**(1–2), 1–16.
12. García, J. C., Gómez, J. M. and Rodríguez, R. C., Rhombohedral–scalenoedral calcite transition produced by adjusting the solution electrical conductivity in the system Ca(OH)₂-CO₂-H₂O. *J. Colloid Interface Sci.*, 2003, **261**(2), 434–440.
13. Boynton, R. S., *Chemistry and Technology of Lime and Limestone*, John Wiley, 1966.
14. Longman, M. W., Carbonate diagenetic textures from nearsurface diagenetic environments. *Am. Assoc. Pet. Geol. Bull.*, 1980, **64**(4), 461–487.
15. Miriello, D. *et al.*, A petrochemical study of ancient mortars from the archaeological site of Kyme (Turkey). *Periodic. Mineral.*, 2015, **84**(3A), 495–517.
16. Binici, H. and Kapur, S., The physical, chemical, and microscopic properties of masonry mortars from Alhambra Palace (Spain) in reference to their earthquake resistance. *Front. Archit. Res.*, 2016, **5**(1), 101–110.
17. Elsen, J., Van Balen, K. and Mertens, G., Hydraulicity in historic lime mortars: a review. In *Historic Mortars*, Springer, 2012, pp. 125–139.
18. Indian Bureau Mines, *Indian Minerals Yearbook 2016*, Government of India, Ministry of Mines, Nagpur, 2018.
19. Kitano, Y., A study of the polymorphic formation of calcium carbonate in thermal springs with an emphasis on the effect of temperature. *Bull. Chem. Soc. Jpn.*, 1962, **35**(12), 1980–1985.
20. Holmes, S. and Wingate, M., *Building with Lime: A Practical Introduction*, ITDG Publishing, London, 1997.
21. Lynch, G., Lime mortars for brickwork: traditional practice and modern misconceptions – part one. *J. Archit. Conserv.*, 1998, **4**(1), 7–20.
22. Erlin, B. and Hime, W. G., Evaluating mortar deterioration. *APT Bull. J. Preserv. Technol.*, 1987, **19**(4), 8–54.
23. Chen, Z. and Nan, Z., Controlling the polymorph and morphology of CaCO₃ crystals using surfactant mixtures. *J. Colloid Interface Sci.*, 2011, **358**(2), 416–422.
24. Ajikumar, P. K., Wong, L. G., Subramanyam, G., Lakshminarayanan, R. and Valiyaveetil, S., Synthesis and characterization of monodispersed spheres of amorphous calcium carbonate and calcite spherules. *Cryst. Growth Des.*, 2005, **5**(3), 1129–1134.
25. Abdelwahab, H. S., *Dictionary in Mineralogy Terms (English–French–Arabic)*, Arab Leag. Educ. Cult. Sci. Organ. Bur. Coord. Arab. Cairo, Egypt, 2003, p. 15.

26. Cazalla, O., Rodriguez-Navarro, C., Sebastian, E., Cultrone, G. and De la Torre, M. J., Aging of lime putty: effects on traditional lime mortar carbonation. *J. Am. Ceram. Soc.*, 2000, **83**(5), 1070–1076.
27. Cultrone, G., Sebastián, E. and Huertas, M. O., Forced and natural carbonation of lime-based mortars with and without additives: mineralogical and textural changes. *Cem. Concr. Res.*, 2005; doi: 10.1016/j.cemconres.2004.12.012.
28. Böke, H., Akkurt, S., İpekoğlu, B. and Uğurlu, E., Characteristics of brick used as aggregate in historic brick-lime mortars and plasters. *Cem. Concr. Res.*, 2006, **36**(6), 1115–1122.
29. Huggett, R., *Fundamentals of Geomorphology*, Routledge, 2007.
30. Inoue, A., Velde, B., Meunier, A. and Touchard, G., Mechanism of illite formation during smectite-to-illite conversion in a hydrothermal system. *Am. Mineral.*, 1988, **73**(11–12), 1325–1334.
31. Roch, G. E., Smiths, M. E. and Drachman, S. R., Solid state NMR characterization of the thermal transformation of an illite-rich clay. *Clays Clay Miner.*, 1998, **46**(6), 694–704.
32. Jung, W. M., Kang, S. H., Kim, W.-S. and Choi, C. K., Particle morphology of calcium carbonate precipitated by gas–liquid reaction in a Couette–Taylor reactor. *Chem. Eng. Sci.*, 2000, **55**(4), 733–747.
33. Tai, C. Y. and Chen, F., Polymorphism of CaCO₃, precipitated in a constant-composition environment. *AIChE J.*, 1998, **44**(8), 1790–1798.
34. Spanos, N. and Koutsoukos, P. G., Kinetics of precipitation of calcium carbonate in alkaline pH at constant supersaturation. Spontaneous and seeded growth. *J. Phys. Chem. B*, 1998, **102**(34), 6679–6684.
35. Dickinson, S. R., Henderson, G. E. and McGrath, K. M., Controlling the kinetic versus thermodynamic crystallisation of calcium carbonate. *J. Cryst. Growth*, 2002, **244**(3–4), 369–378.
36. Weiss, I. M., Tuross, N., Addadi, L. I. A. and Weiner, S., Mollusc larval shell formation: amorphous calcium carbonate is a precursor phase for aragonite. *J. Exp. Zool.*, 2002, **293**(5), 478–491.
37. Singh, M., Kumar, S. V. and Sabale, P. D., Chemical and mineralogical investigations of lime plasters of medieval structures of Hampi, India. *Int. J. Archit. Herit.*, 2019, **13**(5), 725–741.
38. Cizer, Ö., Rodriguez-Navarro, C., Ruiz-Agudo, E., Elsen, J., Van Gemert, D. and Van Balen, K., Phase and morphology evolution of calcium carbonate precipitated by carbonation of hydrated lime. *J. Mater. Sci.*, 2012, **47**(16), 6151–6165.
39. Singh, M., Vinodh Kumar, S., Waghmare, S. A. and Sabale, P. D., Aragonite-vaterite-calcite: polymorphs of CaCO₃ in 7th century CE lime plasters of Alampur group of temples, India. *Constr. Build. Mater.*, 2016, **112**; doi:10.1016/j.conbuildmat.2016.02.191.
40. Selvaraj, T. and Ramadoss, R., Analysis and characterisation of third century ancient mortars at Subramanyaswamy Temple rediscovered after the 2004 tsunami near Mamallapuram shore, India. *Int. J. Conserv. Sci.*, 2018, **9**(1), 2238–2246.
41. Koga, N., Kasahara, D. and Kimura, T., Aragonite crystal growth and solid-state aragonite–calcite transformation: a physico-geometrical relationship via thermal dehydration of included water. *Cryst. Growth Des.*, 2013, **13**(5), 2238–2246.
42. Moropoulou, A., Bakolas, A. and Bisbikou, K., Characterization of ancient, Byzantine and later historic mortars by thermal and X-ray diffraction techniques. *Thermochim. Acta*, 1995, **269**, 779–795.

ACKNOWLEDGEMENT. We thank the Vice-Chancellor, National Museum Institute, New Delhi for support; Dr L. P. Singh, CBRI, Roorkee, and Advanced Instrumentation Centre, IIT, Delhi, for help in the analysis and Pankaj Bijalwan for assistance.

Received 15 May 2021; accepted 6 July 2022

doi: 10.18520/cs/v123/i6/804-813